Forschung im Ingenieurwesen (2024)88:33
https://doi.org/10.1007/s10010-024-00753-3

ORIGINALARBEITEN/ORIGINALS

Thermo-mechanical investigation of a friction oscillator under high-frequency excitation

Simon Keller[1] · **Alexander Fidlin**[1]

Received: 8 March 2024 / Accepted: 17 June 2024

Abstract

The frictional behavior, temperature evolution, and system dynamics in tribological systems are closely coupled. However, in many cases, at least one of the mentioned phenomena is neglected or not modeled consistently. This paper presents a model of a thermo-mechanically coupled oscillator, where the reduction of friction force due to high-frequency excitation is analyzed. The oscillator's equation of motion, the impulse balance, and the heat equation for the thermo-mechanical continuum are evaluated so that a set of nonlinear equations describes the coupled system. Using specific mathematical procedures like Laplace-transformation and a particular transformation ansatz for integral equations, the system can be transformed into a set of ordinary differential equations, enabling efficient simulation. Based on this equation set, an averaging method is applied to eliminate the fast time scale of the mechanical oscillation due to high-frequency excitation so that only the averaged influence of the motion goes into the heat evolution. This procedure leads to concise expressions to determine the stationary state of the system, and the quantities of interest can be calculated conveniently. These equations yield parameter combinations where the friction force can be reduced due to the high-frequency excitation, even though thermal expansion is considered. However, there are also parameter regions where the excitation yields a significantly larger friction force.

Thermomechanische Betrachtung eines Reibschwingers unter hochfrequenter Anregung

Zusammenfassung

In tribologischen Systemen sind das Reibverhalten, die Temperaturentwicklung und die Systemdynamik eng gekoppelt. In vielen Fällen wird allerdings mindestens eins der genannten Phänomene vernachlässigt oder nicht konsistent modelliert. In der vorliegenden Arbeit wird ein Modell eines thermomechanisch gekoppelten Reibschwingers vorgestellt, bei dem die Reibkraftreduktion durch hochfrequente Anregung untersucht wird. Die Bewegungsgleichung des mechanischen Schwingers, die Impulsbilanz und die Wärmeleitungsgleichung des Kontinuums werden ausgewertet, sodass ein System gekoppelter Gleichungen das Systemverhalten beschreibt. Mithilfe der Laplace-Transformation und eines speziellen Transformationsansatzes für Integralgleichungen kann das System durch gekoppelte, gewöhnliche Differentialgleichungen beschrieben werden, was eine effiziente Simulation erlaubt. Ausgehend von diesem Differentialgleichungssystem wird durch ein Mittelwertbildungsverfahren die schnelle Zeitskala der hochfrequenten mechanischen Schwingung eliminiert, sodass nur der gemittelte Einfluss der Bewegung in die Wärmegleichung eingeht. Dies führt zu prägnanten Gleichungen für den stationären Zustand des Systems sowie für die Zielgrößen. Das Lösen dieser Gleichungen liefert Parameterkombinationen, bei denen die Reibkraft durch die hochfrequente Anregung trotz thermischer Ausdehnung reduziert wird. Es gibt allerdings auch Parameterbereiche, bei denen die hochfrequente Anregung aufgrund der thermischen Kopplung zu deutlich größeren Reibkräften führt.

✉ Simon Keller
simon.keller@kit.edu

Alexander Fidlin
alexander.fidlin@kit.edu

[1] Institut für Technische Mechanik Abteilung Dynamik/Mechatronik, Karlsruher Institut für Technologie, 76131 Karlsruhe, Germany

Published online: 25 July 2024

1 Introduction

The effect of fast oscillations on the dynamics of frictional systems has been widely investigated in the last decades. The famous publication of Thomsen [1] deals with quenching friction-induced oscillations using high-frequency excitation. Applying the averaging method, friction-induced oscillations and the stabilizing influence of superposed oscillations are explained and discussed: Due to the smoothening of dry friction, the stable limit cycle with high amplitudes is eliminated, and a new, stable quasi-equilibrium is created. Many publications followed, and the theory was extended towards MDOF systems like the mode-coupling model in [2, 3] or multiple bodies on an evolving belt [4]. It could be shown that high-frequency excitation also has a stabilizing effect on systems with multiple degrees of freedom. In [5, 6], this effect was also shown when the excitation acts in the tangential or normal direction. More complex contact models were applied [7], and experiments were made, which show good accordance with simulation results [8]. The main result of these publications is that by superposing fast oscillations, the characteristics of the destabilizing, discontinuous friction force are changed in such a way that the effective friction force on a slow timescale is continuous and has a damping character, which can yield a stable equilibrium point.

The interaction between dry friction and temperature evolution was investigated in [9] to improve the design of dry journal bearings. The analytical model was refined in [10] and experiments verified the simulated results. In [11], the authors outlined the important influence of the thermal and thermo-mechanical phenomena on the tribological behavior of the system experimentally. Many more publications go into detail in modeling the contact incorporating thermo-mechanics on a microscale [12, 13].

In [14], a one-degree-of-freedom oscillator with velocity- and temperature-dependent friction is analytically investigated. It outlines how the friction temperature and the friction velocity slopes influence the stability of the equilibrium point. The authors of [15–17] combined a friction oscillator with a thermoelastic continuum and investigated the coupling influence on steady-state solution stability and self-excited oscillations due to friction. In [18], the fully coupled system is analyzed concerning chaotic motions. With their models and respective mathematical methods, the interaction between solid body motion, heat evolution, and friction behavior was investigated, and interesting results concerning different types of motion were delivered. These papers partly guide the models and methods used in the present paper.

This publication aims to develop a model that allows for investigating the influence of heat generation on the dynamical and tribological behavior of dry friction bearing under high-frequency excitation, which is especially important for constraint contact conditions. This model should give insight into how a dry journal bearing, which is excited in the axial direction to quench friction-induced phenomena, is influenced by the heat evolution and the accompanying thermal expansion of the shaft, which leads to higher contact pressure and friction forces. The high-frequency excitation will lead to a higher temperature and a higher contact pressure and friction force. The question is then whether the advantages of high-frequency excitation still exist under the thermo-tribological aspect.

The paper is structured as follows: The model under consideration and respective assumptions are explained. Non-dimensional parameters are introduced, and coupled equations describing the full system dynamics are derived. Numerical solutions of the full system are presented. Afterward, an averaging method is used to eliminate the fast time scale, yielding decoupled, autonomous equations for the heat evolution on the slow time scale. Based on these averaged equations, the system's stationary state can be determined for various parameters. The paper concludes with a summary of the most important results. This publication builds upon [19] but extends the model towards considering the initial temperature and respective results.

2 Modelling

The model in Fig. 1 is considered to investigate the influence of high-frequency excitation on the frictional behavior of an oscillator with thermo-mechanical coupling.

A shaft with the axial degree of freedom $\widetilde{x}$ is connected to a wall with a spring and a damper. The block is in tangential contact with the environment, rotating at a constant velocity $\widetilde{v}_0 > 0$. The friction coefficient μ between the rotating environment and the shaft is assumed to be constant. The periodic force $F(t)$ acts in the axial direction and represents the axial high-frequency excitation of the shaft. The equation of motion is given by

$$m\widetilde{x}_{,tt} + d\widetilde{x}_{,t} + c\widetilde{x} + F_\mathrm{a} = \widehat{F}\cos\Omega t\ . \tag{1}$$

In this ordinary differential equation (ODE), F_a describes the Coulomb friction force acting on the shaft in the axial direction

$$F_\mathrm{a} = \mu N\left(\widetilde{T}\right)\frac{\widetilde{x}_{,t}}{\sqrt{\widetilde{x}_{,t}^2 + \widetilde{v}_0^2}} \tag{2}$$

where the normal force $N\left(\widetilde{T}\right)$ is a function of the temperature field $\widetilde{T}(r,t)$ within the shaft. The quantity of interest of this problem is the friction force in the circumferential di-

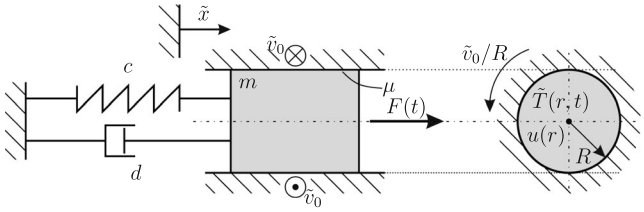

Fig. 1 Model under investigation: single mass oscillator with displacement and temperature field

rection F_c that must be overcome to maintain the prescribed rotation $\widetilde{v}_0$. This quantity is given by the expression

$$F_c = \mu N\left(\widetilde{T}\right)\frac{\widetilde{v}_0}{\sqrt{\widetilde{x}_{,t}^2+\widetilde{v}_0^2}} \tag{3}$$

and depends on the temperature $\widetilde{T}$ and the velocity $\widetilde{x}_{,t}$. The objective is to analyze how the high-frequency excitation influences the friction force F_c and if it causes smaller or larger values compared to the friction force without excitation F_c^0 with

$$F_c^0 = \mu N\left(\widetilde{T}\right) . \tag{4}$$

It is assumed that the shaft remains in permanent contact with the rotating environment independent of the thermal expansion. The press fit has the initial measure u_0, and there is perfect contact around the circumference. For the stress field, a simple Hook's law is applied, where lateral contraction is neglected:

$$\boldsymbol{\sigma} = E\left(\boldsymbol{\varepsilon} - \alpha_e\widetilde{T}\mathbf{1}\right) . \tag{5}$$

The parameter E is the Young's modulus, and $\mathbf{1}$ is the identity matrix. The strain tensor $\boldsymbol{\varepsilon}$ contains the strains in polar coordinates of the rotationally symmetrical displacement field $u(r)$. The parameter α_e describes the material's thermal expansion coefficient, and the function $\widetilde{T}$ describes the temperature difference between the shaft and the environment whose temperature is assumed to remain constant at $\widetilde{T}_0$. The quasi-static balance of momentum reads

$$\mathrm{div}\boldsymbol{\sigma} = \vec{0} . \tag{6}$$

The resulting ODE for the displacement field $u(r)$ is

$$\frac{\partial}{\partial r}\left(\frac{\partial u}{\partial r}+\frac{u}{r}-\alpha_e\widetilde{T}\right) = 0 \tag{7}$$

with the boundary conditions

$$u(R) = -u_0 , \qquad u(0) = 0 . \tag{8}$$

Eq. (7) can be solved analytically and can be used to calculate the contact pressure between the mass block and environment

$$\begin{aligned} p_c &= -\sigma_{rr}(R) \\ &= E\alpha_e\frac{2}{R^2}\int_0^R\widetilde{T}(r,t)r\,\mathrm{d}r + E\frac{u_0}{R} \\ &= E\left(\alpha_e\widetilde{T}_m+\frac{u_0}{R}\right) \end{aligned} \tag{9}$$

where

$$\widetilde{T}_m = \frac{2}{R^2}\int_0^R\widetilde{T}(r,t)r\,\mathrm{d}r \tag{10}$$

is the time-dependent mean temperature over the cross-section of the mass block. Therefore, the expression for the normal force in Eq. (1) is given by

$$N\left(\widetilde{T}\right) = Ap_c = AE\left(\alpha_e\widetilde{T}_m+\frac{u_0}{R}\right) , \tag{11}$$

where A is the contact area.

In the next step, the mean temperature $\widetilde{T}_m$ has to be found by evaluating the heat equation

$$\widetilde{T}_{,t} = \kappa\left(\widetilde{T}_{,rr}+\frac{1}{r}\widetilde{T}_{,r}\right) , \tag{12}$$

where $\widetilde{T} = \widetilde{T}(r,t)$ is the rotationally symmetric temperature field of the shaft, and κ is the thermal diffusivity. The initial condition is

$$\widetilde{T}(r,0) = \widetilde{T}_0 , \tag{13}$$

the boundary conditions read

$$\lim_{r\to 0}(r\,T_{,r}(r,t)) = 0 , \tag{14}$$

$$k\widetilde{T}_{,r}(R,t)+\alpha_T\widetilde{T}(R,t) = \mu\eta p_c\widetilde{v}_{rel} . \tag{15}$$

Eq. (15) describes the heat flow at the interface between the shaft and environment. The flow depends on the temperature difference between the shaft and the environment. Furthermore, there is a heat source describing the effect of friction. The coefficient k is for the thermal conductivity, α_T is for the transport of heat over the interface, μ is the friction coefficient, η is a dimensionless parameter describing how much of the friction power goes into heat,

and $\widetilde{v}_{\mathrm{rel}} = \sqrt{\widetilde{x}_{,t}^2 + \widetilde{v}_0^2}$ is the relative velocity in the contact. A heat flow in the axial direction is not considered.

In the next step, the following dimensionless parameters are introduced:

$$
\begin{aligned}
\tau &= \omega_0 t & \omega_0^2 &= \frac{c}{m} \\
\frac{\partial}{\partial t} &= \omega_0 \frac{\partial}{\partial \tau} = \omega_0 (\dot{}) & x &= \frac{\widetilde{x}}{R} \\
\varrho &= \frac{r}{R} & \frac{\partial}{\partial r} &= \frac{1}{R}\frac{\partial}{\partial \varrho} = \frac{1}{R}(\,)' \\
T &= \frac{\widetilde{T}}{T_*} & \varepsilon &= \frac{\kappa}{\omega_0 R^2} \\
Bi &= \frac{\alpha_{\mathrm{T}} R}{k} & C_0 &= \frac{u_0}{R\alpha_{\mathrm{e}} T_*} \\
T_{\mathrm{m}} &= \frac{\widetilde{T}_{\mathrm{m}}}{T_*} & \gamma &= \frac{E\alpha_{\mathrm{e}} R^2 \omega_0}{k} \\
\widehat{p} &= \frac{AE\alpha_{\mathrm{e}} T_*}{cR} & \widehat{f} &= \frac{\widehat{F}}{cR} \\
\omega &= \frac{\Omega}{\omega_0} & v_{\mathrm{rel}} &= \frac{\widetilde{v}_{\mathrm{rel}}}{\omega_0 R} \\
D &= \frac{d}{2m\omega_0} & v_0 &= \frac{\widetilde{v}_0}{\omega_0 R} \\
T_0 &= \frac{\widetilde{T}_0}{T_*} & f_{\mathrm{c}} &= \frac{F_{\mathrm{c}}}{cR}\,.
\end{aligned}
$$

The characteristic nondimensional parameters are ε, describing the ratio of the time constants of the oscillation and the thermal problem, Bi, describing the ratio of thermal conduction resistance inside the body over the conduction resistance over the boundary surface. The parameter C_0 is a measure for the press fit, γ describes the rise of the contact pressure due to thermal expansion, $\widehat{p}$ is the reference pressure, $\widehat{f}$ and ω being the amplitude and the frequency of the excitation. The heat equation with the respective initial and boundary conditions can then be written as

$$
\dot{T} = \varepsilon \left(T'' + \frac{1}{\varrho} T' \right), \qquad T(\varrho, 0) = T_0\,, \tag{16}
$$

$$
T'(1,\tau) + BiT(1,\tau) = q(\tau)\,, \quad \lim_{\varrho \to 0} (\varrho T'(\varrho,\tau)) = 0\,, \tag{17}
$$

where $q(\tau) = \mu\eta\gamma v_{\mathrm{rel}} (C_0 + T_{\mathrm{m}})$ is the heat source due to the friction power. Applying a Laplace transform to the Eqs. (16) and (17) with

$$
\mathcal{L}\{\cdot\} = \int_0^\infty (\cdot)\exp(-s\tau)\mathrm{d}\tau = \bar{(\cdot)} \tag{18}
$$

yields an ODE of the Bessel kind

$$
\bar{T}'' + \frac{1}{\varrho}\bar{T}' - \frac{s}{\varepsilon}\bar{T} = -\frac{T_0}{\varepsilon}\,, \tag{19}
$$

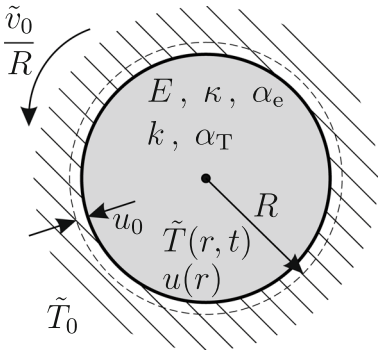

Fig. 2 Thermomechanical continuum with press fit and rotating environment

where $\bar{T} = \bar{T}(\varrho, s)$ is the Laplace transform of the temperature field $T(\varrho, t)$. Eq. (19) can be solved analytically in the frequency domain, where the solution satisfying the boundary conditions is according to [20] as follows:

$$
\bar{T}(\varrho, s) = \frac{I_0\left(\sqrt{\frac{s}{\varepsilon}}\varrho\right)(s\bar{q}(s) - BiT_0)}{s\left(\sqrt{\frac{s}{\varepsilon}} I_1\left(\sqrt{\frac{s}{\varepsilon}}\right) + BiI_0\left(\sqrt{\frac{s}{\varepsilon}}\right)\right)} + \frac{T_0}{s} \tag{20}
$$

where s is the frequency parameter, and $I_0(s)$, $I_1(s)$ are modified Bessel functions of order zero and one. With this expression, the mean temperature $\bar{T}_{\mathrm{m}}$ in the frequency domain can be calculated by

$$
\begin{aligned}
\bar{T}_{\mathrm{m}}(s) &= 2\int_0^1 \bar{T}(\varrho, s)\varrho\mathrm{d}\varrho \\
&= \frac{2I_1\left(\sqrt{\frac{s}{\varepsilon}}\right)(s\bar{q}(s) - BiT_0)}{s\sqrt{\frac{s}{\varepsilon}}\left(\sqrt{\frac{s}{\varepsilon}} I_1\left(\sqrt{\frac{s}{\varepsilon}}\right) + BiI_0\left(\sqrt{\frac{s}{\varepsilon}}\right)\right)} + \frac{T_0}{s} \\
&= \bar{G}_{\mathrm{m},q}(s)\bar{q}(s) + \bar{G}_{\mathrm{m},0}(s)T_0\,.
\end{aligned} \tag{21}
$$

The inverse Laplace transform yields

$$
\begin{aligned}
T_{\mathrm{m}}(\tau) &= \mathcal{L}^{-1}\left\{\bar{T}_{\mathrm{m}}(s)\right\} \\
&= \int_0^\tau G_{\mathrm{m},q}(\tau - y)q(y)\mathrm{d}y + G_{\mathrm{m},0}(\tau)T_0
\end{aligned} \tag{22}
$$

with

$$
q(\tau) = \mu\eta\gamma\sqrt{\dot{x}(\tau)^2 + v_0^2}\,(C_0 + T_{\mathrm{m}}(\tau))\,. \tag{23}
$$

The functions $G_{\mathrm{m},q}(\tau) = \mathcal{L}^{-1}\left\{\bar{G}_{\mathrm{m},q}(s)\right\}$ and $G_{\mathrm{m},0}(\tau) = \mathcal{L}^{-1}\left\{\bar{G}_{\mathrm{m},0}(s)\right\}$ can be found by the use of the residue theorem (cf. Appendix 1), giving

$$
G_{\mathrm{m},q}(\tau) = \sum_{n=1}^{\infty} \beta_n \exp\left(-\varepsilon\lambda_n^2\tau\right) \tag{24}
$$

$$
G_{\mathrm{m},0}(\tau) = Bi\sum_{n=1}^{\infty} \frac{\beta_n}{\lambda_n^2}\exp\left(-\varepsilon\lambda_n^2\tau\right) \tag{25}
$$

where the eigenvalues λ_n and the coefficients β_n can be calculated by

$$Bi J_0(\lambda_n) - \lambda_n J_1(\lambda_n) = 0 \tag{26}$$

$$\text{and} \quad \beta_n = \frac{4Bi}{Bi^2 + \lambda_n^2} . \tag{27}$$

As the functions $G_{\mathrm{m},q}(\tau)$ and $G_{\mathrm{m},0}(\tau)$ have similar coefficients and exponents, Eq. (22) can also be written as

$$T_{\mathrm{m}}(\tau) = \int_0^\tau G_{\mathrm{m},q}(\tau - y)\,(q(y) - \varepsilon Bi T_0)\,\mathrm{d}y + T_0 . \tag{28}$$

Eq. (28) is a Volterra integral equation for the mean temperature $T_{\mathrm{m}}(\tau)$ which is nonlinearly coupled with the velocity $\dot{x}(\tau)$ of the mechanical oscillator through the heat generation term (23). The equation of motion of the oscillator in dimensionless form is

$$\ddot{x} + 2D\dot{x} + x + \widehat{p}\mu\,(C_0 + T_{\mathrm{m}})\,\frac{\dot{x}}{\sqrt{\dot{x}^2 + v_0^2}} = \widehat{f}\cos\omega\tau , \tag{29}$$

where the last part on the left-hand side results from the friction force due to the press fit (C_0) and the enlarged normal force due to the thermal expansion (T_{m}). The friction force of interest f_{c} can be rearranged to

$$f_{\mathrm{c}} = \widehat{p}\mu\,(C_0 + T_{\mathrm{m}})\,\frac{v_0}{\sqrt{\dot{x}^2 + v_0^2}} . \tag{30}$$

To solve the coupled Eqs. (23), (28) and (29) efficiently, they have to be of the same form, either an integral equation or a differential equation. Since solving a system of ODEs is much easier due to sophisticated solvers available in many software packages, Eq. (28) is transformed into a system of ODEs. The function T_{m} is written as a sum of N_{ev} functions and the initial temperature T_0, where N_{ev} is the amount of the computed eigenvalues in Eq. (24), cf. [21, Chap. 6] respective Appendix 1,

$$T_{\mathrm{m}} = \sum_{n=1}^{N_{\mathrm{ev}}} F_n + T_0 , \tag{31}$$

where

$$F_n = \int_0^\tau \beta_n \exp\left(-\varepsilon\lambda_n^2(\tau - y)\right)(q(y) - \varepsilon Bi T_0)\,\mathrm{d}y \tag{32}$$

holds. Differentiating with respect to time τ, applying the Leibniz integral rule and using definition (31) yields the coupled system

$$\begin{aligned} &\dot{F}_n = \beta_n\,(q(\tau) - \varepsilon Bi T_0) - \varepsilon\lambda_n^2 F_n , \\ &F_n(0) = 0 , \quad n = 1 \ldots N_{\mathrm{ev}} , \end{aligned} \tag{33}$$

where Eq. (23) and the assumption (31) hold. It has to be emphasized that the initial temperature T_0 appears in the differential Eq. (33) and the definition (31), whereas the initial condition for the functions F_n are always zero. The transformation allows the equations describing the full, coupled system dynamics to be written as a first-order ODE system.

3 Results

After assigning numerical values to the nondimensional parameters, Eqs. (33) and (29) with respective initial conditions can be solved numerically. The solver `ode45` from MatLab (MathWorks) with a relative and absolute error tolerance of 10^{-8} is used for the following results.

3.1 Full system

A generic solution of the full system can be seen in Fig. 3.

The figure depicts the evolution of the position, the velocity of the shaft, and the mean temperature over time. For a transient time in the beginning, the temperature rises, and the amplitude of the oscillation decays. Afterward, a stationary state is reached, where the shaft's motion is periodic, and the temperature fluctuates around a constant value. It is essential to mention that even though there is no damping ($D = 0$) and the excitation is in resonance ($\omega = 1$), the amplitude of the oscillations is bounded. The temperature rises while the oscillation amplitude decays until an equilibrium is established even for higher excitation amplitudes. During this transient time interval, energy in the form of heat flows into the shaft, the temperature rises, and the shaft expands thermally. In the stationary state, the mean energy of the shaft remains constant. The input energy is the same as the energy that flows over the boundary into the environment, which acts as a heat sink. In Fig. 4, the friction force in the circumferential direction is depicted for the system with and without excitation ($\widehat{f} = 0$).

If the shaft is not excited, the temperature and therefore the friction force still rises due to the heat source caused by the prescribed rotation v_0. As can be seen, the stationary value without excitation is about 15% greater than the average value with excitation. For this parameter set, the high-frequency excitation leads to a reduced friction force even when the coupling with thermal expansion is considered.

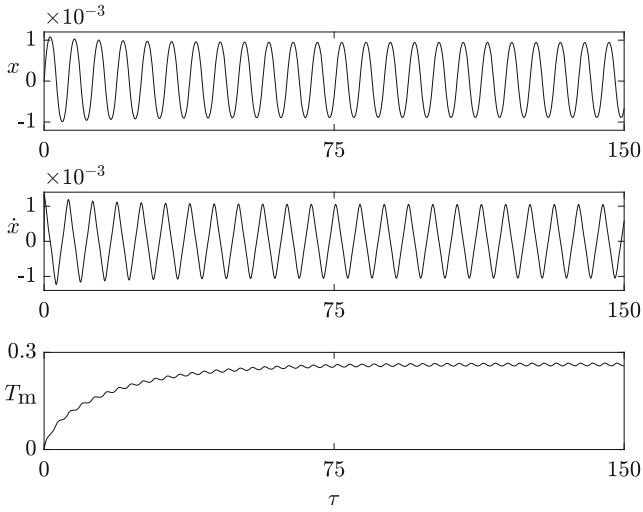

Fig. 3 Generic solution for the following parameters: $\widehat{f} = 20$, $\omega = 1$, $D = 0$, $v_0 = 0.001$, $\gamma = 100$, $\varepsilon = 0.01$, $Bi = 20$, $\eta = 0.8$, $\mu = 0.2$, $C_0 = 2.5$, $\widehat{p} = 50$, $T_0 = 0$, and $N_{\mathrm{ev}} = 10$

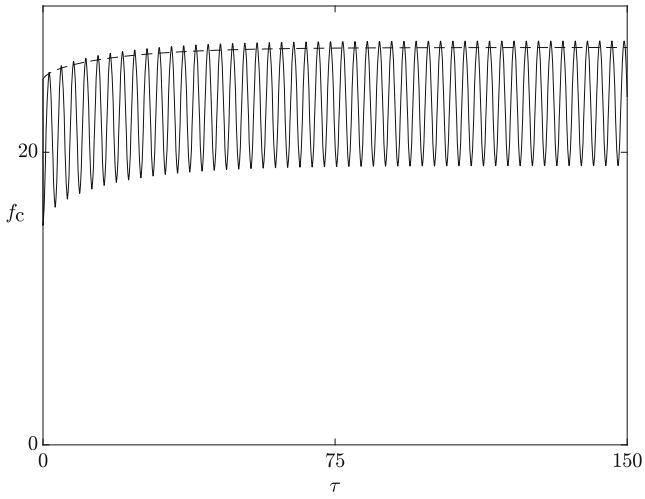

Fig. 4 Comparison of circumferential friction force with (–) and without excitation (- -), for the solution in Fig. 3

3.2 Averaged system

In the evolution of T_{m} in Fig. 3, one can observe that there seem to be two different time scales: A slow transient behavior of exponential type is superposed by a high-frequency fluctuation with a small amplitude. The slow part origins from the nature of heat conduction, whereas the fast oscillating part results from the heat generation through the oscillating shaft. The aim is now to investigate the averaged influence of the heat source on the temperature evolution. The idea is to find a solution of the equation of motion (29) in dependence of the mean temperature T_{m}, assuming it to be a constant parameter, substitute this into the equation for the heat evolution (Eq. (22) respective (23)) and average this equation over one period of the fast time scale of the mechanical oscillation. This results in an equation that describes the system behavior on the slow time scale. This procedure is based on the idea of Blekhman in [22].

By investigating the numerical results of the full system, one can observe that the contribution of the inertia, damping, and spring forces in Eq. (29) is very small compared to the friction force and the excitation. The friction force seems to be dominant, so that inertia, damping, and spring force terms can be neglected, which gives the new equation

$$\widehat{p}\mu\,(C_0 + T_{\mathrm{m}})\,\frac{\dot{x}}{\sqrt{\dot{x}^2 + v_0^2}} = \widehat{f}\cos\omega\tau\ . \tag{34}$$

This equation can be solved for $\dot{x}^2$, which can then be rewritten as

$$\sqrt{\dot{x}^2 + v_0^2} = v_0 \frac{1}{\sqrt{1 - \left(\frac{\widehat{f}}{\widehat{p}\mu(C_0+T_{\mathrm{m}})}\right)^2 \cos^2\omega\tau}}\ . \tag{35}$$

This simplification is only valid, when $\mu\widehat{p}(C_0 + T_{\mathrm{m}}) > \widehat{f}$ holds. In the physical sense, this inequality implies that the friction force must permanently be larger than the excitation amplitude. This requirement can be met by choosing an appropriate initial temperature T_0. Otherwise, the averaging method cannot be applied. By substituting Eq. (35) into Eq. (33), the resulting expression is

$$\begin{aligned}\dot{F}_n = \beta_n\mu\eta\gamma v_0 &\frac{1}{\sqrt{1 - \left(\frac{\widehat{f}}{\widehat{p}\mu(C_0+\sum F_j+T_0)}\right)^2 \cos^2\omega\tau}} \\ &\cdot \left(C_0 + \sum_{j=1}^{N_{\mathrm{ev}}} F_j + T_0\right) - \varepsilon Bi T_0 - \varepsilon\lambda_n^2 F_n\ .\end{aligned} \tag{36}$$

This equation does not contain the function $x(\tau)$ or its derivatives, so the system is now decoupled. As a next step, we can see that the slow functions F_n as well as the fast function $\cos\omega\tau$ are still present. As the functions F_n are assumed to change slowly during one period of the fast function $\cos\omega\tau$, they are kept constant during an averaging

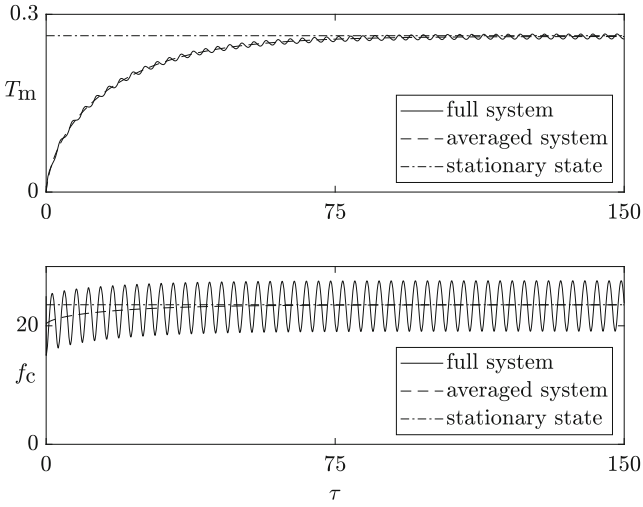

Fig. 5 Comparison of the full model with the averaged model and the stationary state, same parameter set as in Fig. 3

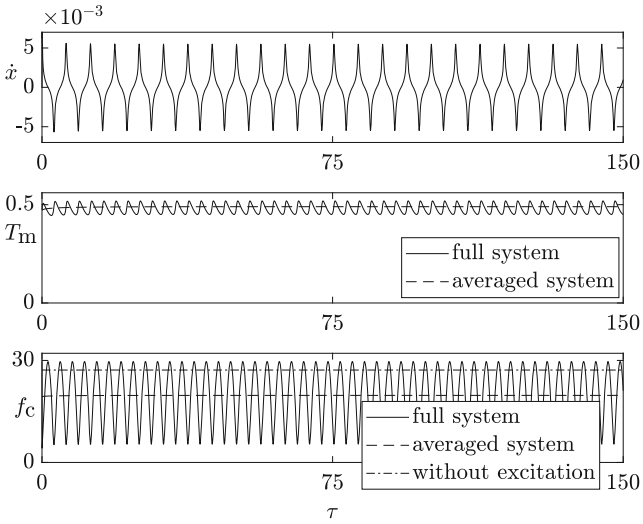

Fig. 6 Comparison of the full model with the averaged model, similar parameter set as in Fig. 3, but with $\widehat{f} = 29.5$ and $T_0 = 0.4725$

of Eq. (36) over one period of the fast oscillation. The averaged equations then read

$$\dot{F}_n = \beta_n \mu \eta \gamma v_0 \frac{2}{\pi} K\left(\frac{\widehat{f}}{\widehat{p}\mu\left(C_0 + \sum F_j + T_0\right)}\right) \cdot \left(C_0 + \sum_{j=1}^{N_{ev}} F_j + T_0\right) - \varepsilon Bi T_0 - \varepsilon \lambda_n^2 F_n \,, \tag{37}$$

where $K(k)$ is the complete elliptic integral of the first kind

$$K(k) = \int_0^{\pi/2} \frac{1}{\sqrt{1 - k^2 \cos^2\theta}} \mathrm{d}\theta \,. \tag{38}$$

A classic averaging method, as explained in [23], with the small parameters ε and v_0 results exactly in the same equations. With this step, the fast time scale is eliminated, and we now have an autonomous system on the slow time scale, which no longer explicitly depends on time. The averaged friction force in circumferential direction f_c can be calculated by

$$f_c = \widehat{p}\mu\left(C_0 + T_m\right) \frac{2}{\pi} E\left(\frac{\widehat{f}}{\widehat{p}\mu\left(C_0 + T_m\right)}\right) \,, \tag{39}$$

and depends only on the mean temperature T_m. The function $E(k)$ is the complete elliptic integral of the second kind

$$E(k) = \int_0^{\pi/2} \sqrt{1 - k^2 \cos^2\theta} \mathrm{d}\theta \,. \tag{40}$$

In Fig. 5, the comparison of the full and averaged system is depicted. As one can see, the full system's solution envelops the averaged system's solution. The accordance is adequate, furthermore, the computational time for the averaged equations is about one order of magnitude smaller. The constant stationary state of the temperature T_m^* and the circumferential friction force f_c^* are also shown, their computation is explained in the next Sect. 3.3.

Fig. 6 shows another plot with velocity, temperature, and friction force over time. The parameters are chosen such that the excitation amplitude $\widehat{f}$ is larger than the static friction force $f_b = \mu \widehat{p} C_0$. The initial temperature T_0 is large enough to apply the averaging procedure. The velocity signal is periodic. After a barely noticeable transient period, the temperature and friction force are also stationary. The averaged solutions for the temperature and the friction force show great accordance with the full system. Furthermore, the friction force is reduced by approximately 20% compared to the friction force without excitation.

3.3 Stationary state

To calculate the stationary temperature $T_m^* = \text{const.}$, one can solve the equation system (37) for $\dot{F}_n = 0$. The division by $\varepsilon \lambda_n^2$ and summing up over the N_{ev} equations delivers

$$T_m^* = \frac{v_0}{v_b} \frac{2}{\pi} K\left(\frac{\widehat{f}}{\widehat{p}\mu\left(C_0 + T_m^*\right)}\right)\left(C_0 + T_m^*\right) \tag{41}$$

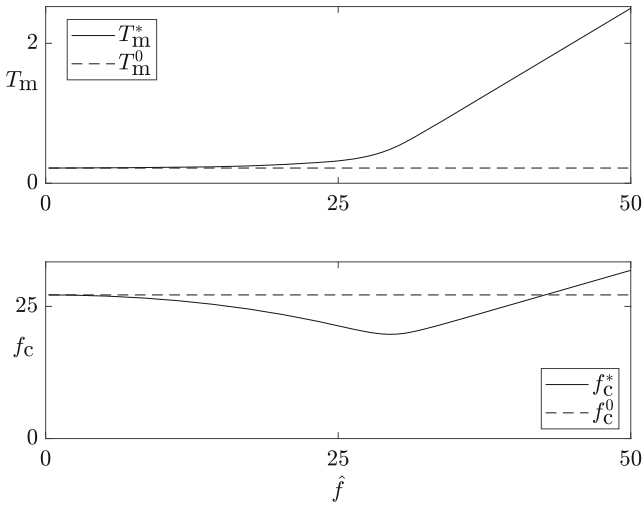

Fig. 7 Stationary temperature and circumferential friction force over excitation amplitude compared to the values without excitation for $v_0 = 0.001$, $\gamma = 100$, $\varepsilon = 0.01$, $Bi = 20$, $\eta = 0.8$, $\mu = 0.2$, $C_0 = 2.5$, $\widehat{p} = 50$. It is $v_0/v_\mathrm{b} = 0.08$ and $f_\mathrm{b} = 25$

where $v_\mathrm{b} = \frac{\varepsilon Bi}{\mu\eta\gamma}$ is a dimensionless boundary velocity and the identity

$$\sum_{n=1}^{\infty} \frac{\beta_n}{\lambda_n^2} = \frac{1}{Bi} \tag{42}$$

is used. The initial temperature T_0 does not influence the stationary state. The stationary circumferential friction force f_c^* can be calculated analogously to Eq. (39) with $T_\mathrm{m} = T_\mathrm{m}^*$. For comparison, the stationary friction force f_c^0 without excitation can be calculated by using Eqs. (44) and (39) with $\widehat{f} = 0$, yielding

$$f_\mathrm{c}^0 = \widehat{p}\mu C_0 \frac{v_\mathrm{b}}{v_\mathrm{b} - v_0} \,. \tag{43}$$

Besides its solution, Eq. (41) offers an interesting insight into the system behavior concerning the existence of the stationary state and the lower limit for the temperature.

If $v_0 > v_\mathrm{b}$, Eq. (41) has no real solution, and therefore no stationary state exists. The physical explanation is that the energy input due to the prescribed motion v_0 is larger than what can flow over the boundary into the environment. In this case, the oscillation amplitude decays asymptotically towards zero, whereas the temperature and friction force rise towards infinity. This case can be interpreted as a thermo-mechanical instability (cf. [24]). Furthermore, Eq. (41) provides a lower limit for the stationary temperature T_m^*. For $\widehat{f} < f_\mathrm{b}$, physical reasons give the simple estimation $T_\mathrm{m}^* > T_\mathrm{m}^0$, the temperature that establishes without excitation. It is

$$T_\mathrm{m}^0 = C_0 \frac{v_0}{v_\mathrm{b} - v_0} \tag{44}$$

that can be evaluated by considering Eq. (41) for $\widehat{f} = 0$. However for $\widehat{f} > f_\mathrm{b}$, the domain of definition of the elliptical integral function $K(k)$ delivers $T_\mathrm{m}^* > \frac{\widehat{f}}{\widehat{p}\mu} - C_0 = C_0 \left(\frac{\widehat{f}}{f_\mathrm{b}} - 1 \right)$ as a lower boundary. The stationary temperature rises linearly with the excitation amplitude, which can be observed in Fig. 7.

Using Eqs. (41) and (39) and the necessary condition for the existence of a stationary state, the system behavior can easily be analyzed for a large variety of parameters by solving the equation numerically. Analyzing the full system would be much more laborious, furthermore, the essential parameter combinations v_b and f_b could not be identified that easily. The boundary velocity v_b limits how large the energy flow out of the shaft can be. The knowledge of the ratio v_0/v_b allows a prediction of whether a stationary state can be reached. In the physical sense, f_b is the static friction force acting on the shaft. If $\widehat{f} < f_\mathrm{b}$, the excitation force is smaller than the static friction force, and the shaft would stick if the environment did not rotate around it, which permanently prevents it from sticking. If $\widehat{f} > f_\mathrm{b}$, the shaft velocity increases rapidly due to the strong excitation force. This leads to a high value for the mean temperature so that $\widehat{f} < f_\mathrm{b} + \widehat{p}\mu T_\mathrm{m}^*$ holds and an equilibrium is established. The stationary temperature can be found by solving Eq. (41) numerically with an appropriate initial guess for T_m^*. With the knowledge of T_m^*, the stationary friction force f_c^* can be calculated. Another interesting system property is that the excitation frequency ω does not affect the stationary state, as seen from the Eq. (41). Although the system contains a mechanical oscillator, the excitation frequency does not influence the stationary temperature, which seems unintuitive. As the heat input depends on the average relative velocity and the oscillation is much faster than the thermal evolution, the excitation frequency vanishes due to the averaging.

In Fig. 7, the stationary temperature T_m^* and the stationary friction force f_c^* are plotted against the excitation amplitude $\widehat{f}$. The dashed line in the upper plot is the constant temperature T_m^0 without excitation and is always smaller than T_m^*. Until $\widehat{f} = f_\mathrm{b}$, the value of T_m^* rises slowly. Afterward, the slope is much steeper and tends towards a straight line with constant inclination. In the second plot in Fig. 7, the stationary circumferential friction force f_c^* is plotted over the excitation amplitude $\widehat{f}$ and compared to the friction force f_c^0 without excitation ($\widehat{f} = 0$). It is interesting to observe that there seems to be an opti-

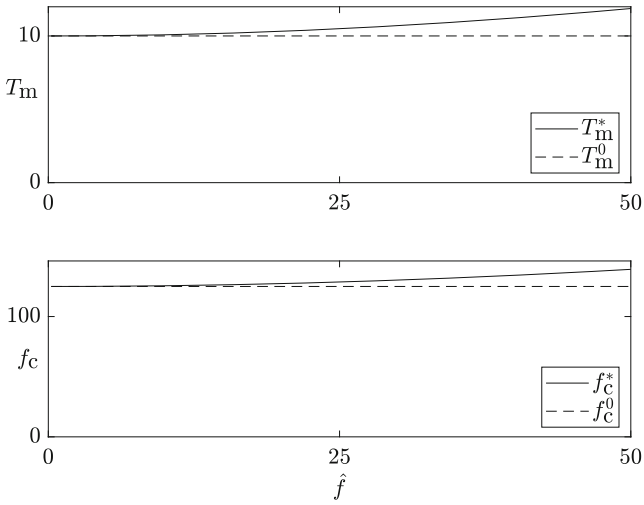

Fig. 8 Stationary temperature and circumferential friction force over excitation amplitude compared to the values without excitation for similar parameters as in Fig. 7 but $v_0 = 0.01$. It is $v_0/v_\mathrm{b} = 0.8$ and $f_\mathrm{b} = 25$

mum where the friction force is minimal. In this case, the minimum is at $\widehat{f} \approx 29.5$ slightly larger than the value $f_\mathrm{b} = 25$. The respective time series is depicted in Fig. 6. With increasing excitation amplitude, the mean temperature and the friction force increase linearly, and the friction reduction effect vanishes. This behavior can be explained by the fact that for increasing excitation amplitude $\widehat{f}$, the oscillator's velocity amplitude increases, which has a smaller friction force as a consequence. However, when $\widehat{f} > f_\mathrm{b}$, the mean temperature increases much faster and the friction force with it.

In Fig. 8, the environment velocity is increased by 10 to $v_0 = 0.01$ compared to Fig. 7. One can observe that the mean temperature and friction force are much higher than in Fig. 7. This can be explained by the increased heat input by the higher velocity v_0. Accordingly, the temperature is higher and, therefore, the friction force. Furthermore, there is no parameter area where the friction force is reduced. That means if v_0 is near v_b, high-frequency excitation negatively influences the system, as the reducing effect is absent and the friction force is even larger than that without excitation.

4 Conclusion

Using a rather simple mechanical model and specific mathematical methods, the influence of the thermo-mechanical coupling on a friction oscillator under high-frequency excitation has been worked out. Based on ordinary and partial differential equations for solid body motion, displacement, and temperature field, an infinite system of coupled ordinary differential equations is derived, which describes the full system dynamics. The existence of a stationary state and the friction reduction due to the external excitation is shown. After considering the numerical results, an averaging method is applied, which eliminates the fast time scale of the mechanical oscillations so that an autonomous system for the slow evolution of the temperature results. The averaged equations show good accordance with the full system and allow the calculation of the stationary state. Besides concise equations for the stationary temperature and friction force, existence conditions and two significant parameters can be found: the boundary velocity v_b and the boundary force f_b. This knowledge can be used to investigate the system efficiently. It is found that a parameter area exists in which the friction force in the circumferential direction can be reduced by high-frequency excitation. However, the thermo-mechanical coupling can also deliver increased friction forces. One determining parameter ratio is v_0/v_b, where v_b is a measure of how large the heat flow inside the continuum and across the boundary into the environment is. The friction force can be reduced if the ratio is much smaller than one. There is no stationary state if it is larger than one, and the temperature and friction force grow towards infinity. The second important parameter ratio is $\widehat{f}/f_\mathrm{b}$, where f_b is the static friction force. The friction force reduction is maximal when the ratio is slightly greater than one. When the ratio is smaller than one, the reducing effect diminishes until it vanishes at $\widehat{f} = 0$. When the ratio is much greater than one, stationary temperature and friction force increase drastically, and the friction-reducing effect is destroyed.

5 Appendix

5.1 Inverse Laplace transformation

In this section, the inverse Laplace transformation for Eq. (24) is shown. This delivers the eigenvalues λ_n and respective coefficients β_n. The procedure is analogous for Eq. (25). The inverse Laplace transformation is defined as

$$G_{\mathrm{m},q}(\tau) = \mathcal{L}^{-1}\left\{\bar{G}_{\mathrm{m},q}(s)\right\} \tag{45}$$

$$= \frac{1}{2\pi i}\int_{a-i\infty}^{a+i\infty} \bar{G}_{\mathrm{m},q}(s)\exp(s\tau)\mathrm{d}s\ , \tag{46}$$

where a is so large that all singularities of $\bar{G}_{\mathrm{m},q}(s)$ lie to the left of the line $(a-i\infty, a+i\infty)$, cf. [20, Chap. 12]. The residue theorem for the function

$$f(s) = \bar{G}_{\mathrm{m},q}(s)\exp(s\tau) \tag{47}$$

gives

$$\frac{1}{2\pi i}\int_{-\infty}^{\infty} f(s)\mathrm{d}s = \sum_{s_n}\mathrm{Res}_{s_n} f(s)\ , \tag{48}$$

where s_n are the singularities of $f(s)$. The function

$$f(s) = \frac{2I_1\left(\sqrt{\frac{s}{\varepsilon}}\right)\exp(s\tau)}{\sqrt{\frac{s}{\varepsilon}}\left(\sqrt{\frac{s}{\varepsilon}}I_1\left(\sqrt{\frac{s}{\varepsilon}}\right) + BiI_0\left(\sqrt{\frac{s}{\varepsilon}}\right)\right)} \tag{49}$$

$$= \frac{f_{\mathrm{N}}(s)}{f_{\mathrm{D}}(s)}\exp(s\tau) \tag{50}$$

is split up into a numerator function

$$f_{\mathrm{N}}(s) = \frac{2I_1\left(\sqrt{\frac{s}{\varepsilon}}\right)}{\sqrt{\frac{s}{\varepsilon}}} \tag{51}$$

and a denominator function

$$f_{\mathrm{D}}(s) = \sqrt{\frac{s}{\varepsilon}}I_1\left(\sqrt{\frac{s}{\varepsilon}}\right) + BiI_0\left(\sqrt{\frac{s}{\varepsilon}}\right)\ . \tag{52}$$

The function $f(s)$ has singularities at the roots of the function $f_{\mathrm{D}}(s)$.The point $s = 0$ is not a singularity, since

$$\lim_{s\to 0} f_{\mathrm{N}}(s) = \lim_{s\to 0}\frac{2I_1\left(\sqrt{\frac{s}{\varepsilon}}\right)}{\sqrt{\frac{s}{\varepsilon}}} = 1\ . \tag{53}$$

As Eq. (52) only has complex roots of first order, the substitution $s = -\varepsilon\lambda^2$ is applied. The modified Bessel functions with complex arguments can be rewritten as Bessel functions, so that the equation

$$BiJ_0(\lambda) - \lambda J_1(\lambda) = 0 \tag{54}$$

can be used to find the countably infinite number of eigenvalues λ_n respective s_n, cf. Eq. (26). The residue of the function $f(s)$ at the singularity s_n can be calculated by

$$\mathrm{Res}_{s_n} f(s) = \lim_{s\to s_n}\left((s-s_n)f(s)\right)\ . \tag{55}$$

This yields

$$\mathrm{Res}_{s_n} f(s) = f_{\mathrm{N}}(s_n)\exp(s_n\tau)\lim_{s\to s_n}\frac{s-s_n}{f_{\mathrm{D}}(s)}\ . \tag{56}$$

As both the numerator $s-s_n$ and the denominator $f_{\mathrm{D}}(s)$ tend towards zero for $s \to s_n$, L'Hopital's rule can be applied, giving

$$\lim_{s\to s_n}\frac{s-s_n}{f_{\mathrm{D}}(s)} = \lim_{s\to s_n}\frac{1}{\frac{\mathrm{d}}{\mathrm{d}s}f_{\mathrm{D}}(s)}\ . \tag{57}$$

Therefore, it is

$$\mathrm{Res}_{s_n} f(s) = \frac{f_{\mathrm{N}}(s_n)\exp(s_n\tau)}{\frac{\mathrm{d}}{\mathrm{d}s}f_{\mathrm{D}}(s)\big|_{s=s_n}}\ , \tag{58}$$

with

$$\frac{\mathrm{d}}{\mathrm{d}s}f_{\mathrm{D}}(s) = \frac{BiI_1\left(\sqrt{\frac{s}{\varepsilon}}\right) + \sqrt{\frac{s}{\varepsilon}}I_0\left(\sqrt{\frac{s}{\varepsilon}}\right)}{2\varepsilon\sqrt{\frac{s}{\varepsilon}}}\ . \tag{59}$$

Substituting $s_n = -\varepsilon\lambda_n^2$ and rewriting the modified Bessel functions finally yields

$$\begin{aligned}\mathrm{Res}_{s_n} f(s) &= \frac{4J_1(\lambda_n)}{BiJ_1(\lambda_n) + \lambda_n J_0(\lambda_n)}\exp(-\varepsilon\lambda_n^2\tau)\\ &= \frac{4Bi}{Bi^2+\lambda_n^2}\exp(-\varepsilon\lambda_n^2\tau)\\ &= \beta_n\exp(-\varepsilon\lambda_n^2\tau)\ ,\end{aligned} \tag{60}$$

with

$$\beta_n = \frac{4Bi}{Bi^2+\lambda_n^2}\ , \tag{61}$$

where the Bessel functions were eliminated using the eigenvalue Eq. (54). Therefore, the inverse Laplace transformation of $\bar{G}_{\mathrm{m},q}(s)$ is given by

$$G_{\mathrm{m},q}(\tau) = \sum_{n=1}^{\infty}\mathrm{Res}_{s_n} f(s) \tag{62}$$

$$= \sum_{n=1}^{\infty}\beta_n\exp(-\varepsilon\lambda_n^2\tau)\ . \tag{63}$$

The same procedure holds for the inverse transformation of $\bar{G}_{\mathrm{m},0}(s)$, where the residues differ slightly.

Funding Open Access funding enabled and organized by Projekt DEAL.

Conflict of interest On behalf of all authors, the corresponding author states that there is no conflict of interest.

References

1. Thomsen J (1999) Using fast vibrations to quench friction-induced oscillations. J Sound Vib 228:1079–1102
2. Hoffmann N, Wagner N, Gaul L (2005) Quenching mode-coupling friction-induced instability using high-frequency dither. J Sound Vib 279:471–480
3. Sahoo P, Chatterjee S (2020) Effect of high-frequency excitation on friction induced vibration caused by the combined action of velocity-weakening and mode-coupling. J Vib Control 26:735–746
4. Keller S, Seemann W (2021) Quenching friction-induced oscillations in multibody-systems by the use of high-frequency excitation. Proc Appl Math and Mech 20. https://doi.org/10.1002/pamm.202000185
5. Popov M, Li Q (2018) Multimode active control of friction, dynamic ratchets and actuators. Phys Mesomech 21:24–31
6. Benad J, Nakano K, Popov VL, Popov M (2019) Active control of friction by transverse oscillations. Friction 7:74–85
7. Tsai C, Tseng C (2006) The effect of friction reduction in the presence of in-plane vibrations. Arch Appl Mech 75:164–176
8. Kapelke S (2019) Zur Beeinflussung reibungsbehafteter systeme mithilfe überlagerter Schwingungen. KIT Scientific Publishing, Karlsruhe
9. Floquet A, Play D, Godet M (1977) Surface temperatures in distributed contacts. application to bearing design
10. Floquet A, Play D (1981) Contact temperature in dry bearings. three dimensional theory and verification. J Lubr Tech. https://citeseerx.ist.psu.edu/document?repid=rep1&type=pdf&doi=ae10646f929f6ed54ff186e9765ec39237d4fad3. Accessed 10 Jul 2024
11. Kennedy FE Jr (1984) Thermal and thermomechanical effects in dry sliding. Wear 100:453–476
12. Oestringer L (2023) Thermomechanischer Kontakt und stochastische Dynamik gleitender Körper mit rauen Oberflächen. KIT Scientific Publishing, Karlsruhe
13. Oestringer L, Proppe C (2022) On the transient thermomechanical contact simulation for two sliding bodies with rough surfaces and dry friction. Tribol Int 170. https://doi.org/10.1016/j.triboint.2021.107425
14. Nosko O (2016) Analytical study of sliding instability due to velocity-and temperature-dependent friction. Tribol Lett 61:1–10
15. Awrejcewicz J, Pyryev Y (2002) Thermoelastic contact of a rotating shaft with a rigid bush in conditions of bush wear and stick-slip movements. Int J Eng Sci 40:1113–1130
16. Awrejcewicz J, Pyryev Y (2005) Thermo-mechanical model of frictional self-excited vibrations. Int J Mech Sci 47:1393–1408
17. Olesiak Z, Pyryev Y (2000) A nonlinear, nonstationary problem of frictional contact with inertia and heat generation taken into account. Acta Mech 143:67–78
18. Awrejcewicz J, Pyryev Y (2003) Influence of tribological processes on a chaotic motion of a bush in a cylinder-bush system. Meccanica 38:749–761
19. Keller, S, Fidlin, A (2023) Thermomechanical investigation of a friction oscillator under high-frequency excitation. VDI-Berichte 2429:171–184
20. Carslaw H, Jaeger J (1997) Conduction of heat in solids, 2nd edn. Oxford science publications. Clarendon Press, Oxford
21. Linz P (1985) *Analytical and numerical methods for Volterra equations* SIAM studies in applied mathematics, 7th edn. Society for Industrial and Applied Mathematics, Philadelphia, Pa.
22. Blekhman I (2000) Vibrational mechanics: nonlinear dynamic effects, general approach, applications. World Scientific
23. Nayfeh AH, Mook DT (1979) *Nonlinear oscillations* pure and applied mathematics. Wiley, New York, Chichester, Brisbane, Toronto
24. Ciavarella M, Johansson L, Afferrante L, Klarbring A, Barber J (2003) Interaction of thermal contact resistance and frictional heating in thermoelastic instability. Int J Solids Struct 40:5583–5597